NATIONAL ADVISORY COMMITTEE FOR AERONAUTICS

REPORT 1320

AN EVALUATION OF FOUR EXPERIMENTAL METHODS FOR MEASURING MEAN PROPERTIES OF A SUPERSONIC TURBULENT BOUNDARY LAYER

By GEORGE J. NOTHWANG

1957

REPORT 1320

AN EVALUATION OF FOUR EXPERIMENTAL METHODS FOR MEASURING MEAN PROPERTIES OF A SUPERSONIC TURBULENT BOUNDARY LAYER

By GEORGE J. NOTHWANG

Ames Aeronautical Laboratory
Moffett Field, Calif.

National Advisory Committee for Aeronautics

Headquarters, 1512 H Street NW., Washington 25, D. C.

Created by Act of Congress approved March 3, 1915, for the supervision and direction of the scientific study of the problems of flight (U. S. Code, title 50, sec. 151). Its membership was increased from 12 to 15 by act approved March 2, 1929, and to 17 by act approved May 25, 1948. The members are appointed by the President and serve as such without compensation.

JAMES H. DOOLITTLE, Sc. D., Shell Oil Company, *Chairman*

LEONARD CARMICHAEL, Ph. D., Secretary, Smithsonian Institution, *Vice Chairman*

ALLEN V. ASTIN, Ph. D., Director, National Bureau of Standards.

PRESTON R. BASSETT, M. A., Vice President, Sperry Rand Corp.

DETLEV W. BRONK, Ph. D., President, Rockefeller Institute for Medical Research.

FREDERICK C. CRAWFORD, Sc. D., Chairman of the Board, Thompson Products, Inc.

WILLIAM V. DAVIS, JR., Vice Admiral, United States Navy, Deputy Chief of Naval Operations (Air).

JEROME C. HUNSAKER, Sc. D., Massachusetts Institute of Technology.

CHARLES J. MCCARTHY, S. B., Chairman of the Board, Chance Vought Aircraft, Inc.

CARL J. PFINGSTAG, Rear Admiral, United States Navy, Assistant Chief for Field Activities, Bureau of Aeronautics.

DONALD L. PUTT, Lieutenant General, United States Air Force, Deputy Chief of Staff, Development.

JAMES T. PYLE, A. B., Administrator of Civil Aeronautics.

FRANCIS W. REICHELDERFER, Sc. D., Chief, United States Weather Bureau.

EDWARD V. RICKENBACKER, Sc. D., Chairman of the Board, Eastern Air Lines, Inc.

LOUIS S. ROTHSCHILD, Ph. B., Under Secretary of Commerce for Transportation.

NATHAN F. TWINING, General, United States Air Force, Chief of Staff.

HUGH L. DRYDEN, PH. D., *Director*

JOHN W. CROWLEY, JR., B. S., *Associate Director for Research*

JOHN F. VICTORY, LL. D., *Executive Secretary*

EDWARD H. CHAMBERLIN, *Executive Officer*

HENRY J. E. REID, D. Eng., Director, Langley Aeronautical Laboratory, Langley Field, Va.

SMITH J. DEFRANCE, D. Eng., Director, Ames Aeronautical Laboratory, Moffett Field, Calif.

EDWARD R. SHARP, Sc. D., Director, Lewis Flight Propulsion Laboratory, Cleveland, Ohio

WALTER C. WILLIAMS, B. S., Chief, High-Speed Flight Station, Edwards, Calif.

REPORT 1320

AN EVALUATION OF FOUR EXPERIMENTAL METHODS FOR MEASURING MEAN PROPERTIES OF A SUPERSONIC TURBULENT BOUNDARY LAYER [1]

By George J. Nothwang

SUMMARY

Surveys were made through a turbulent boundary layer on a flat plate by means of a pitot probe, an X-ray densitometer, and hot-wire and cold-wire probes. Results from these surveys were analyzed to determine (a) the reliability of the basic data and hence the methods by which they were obtained, and (b) how well the actual distributions of properties in the boundary layer compare with those commonly assumed in semiempirical and theoretical analyses. All surveys were made at the same longitudinal station on the flat plate. The tests were conducted in an 8- by 8-inch supersonic nozzle. The free-stream Mach number was 3.03 and the Reynolds number was approximately 210,000 based on boundary-layer thickness.

Analysis of the data revealed the following points. The values of mean pitot pressure, mean density, and mean total temperature obtained from the pitot probe, X-ray densitometer, and cold-wire probe combined to produce consistent distributions of mean Mach number, mean total temperature, and mean mass flow throughout the boundary layer. However, mean mass flows computed from these data do not include the effects of combined density and velocity fluctuations and, hence, they can be in error for the supersonic turbulent boundary layer. The hot-wire probe indicated values of mean mass flow over the outer portion of the boundary layer that were higher than the values obtained from the pitot, X-ray, and cold-wire surveys. This result was confirmed in an independent test performed at a Mach number of 1.95 in the Ames 1- by 3-foot supersonic wind tunnel. It is suggested that corrections to hot-wire data may be required to obtain the true mass flows in turbulent supersonic boundary layers.

Except for the region very near the plate surface, the assumption of constant total temperature through the boundary layer yielded negligible errors in velocity distribution, and displacement and momentum thicknesses. The one-sixth power law was found to agree with the experimental velocity distribution within ±2 percent.

INTRODUCTION

Experimental surveys of turbulent boundary layers have, for the most part, been made with pitot probes. There has been, however, some doubt as to whether the probes disturb the boundary layer appreciably (see ref. 1), and moreover, as to whether or not they yield an accurate value of mean pitot pressure when located in a highly turbulent stream

(ref. 2). Furthermore, when the distribution of pitot pressure through the compressible turbulent boundary layer has been determined, distributions of one or more of the other properties in the boundary layer must usually be assumed before all desired information can be obtained. For example, the computation of velocity distribution using data from a pitot survey requires assumed distributions of (a) total temperature through the boundary layer and (b) static pressure through the boundary layer.

Other experimental techniques have, of course, been used to provide information on boundary layers. The X-ray absorption method has, for example, provided mean density distributions (ref. 3), whereas surveys using hot-wire probes have yielded mean mass-flow distributions (ref. 4). Also, cold-wire surveys have been made to obtain mean total-temperature distributions.

With each of these techniques there has, as with the pitot survey method, been some question as to the reliability of the data obtained. This fact has, of course, been recognized and subjected to some study (ref. 3). There is one test of reliability which has not, however, to the knowledge of the author been performed. This test consists of studying the same boundary layer with all four of the techniques mentioned. Various combinations of the resulting basic data could then be used to obtain distributions of a particular property in the boundary layer. Agreement (or disagreement) in the values obtained for this property would provide the check on reliability of the techniques. A check of assumptions commonly used in boundary-layer analyses (such as constant total temperature) could, of course, be a valuable by-product of this investigation. These considerations prompted the author to carry out just such an investigation of a turbulent boundary layer on an essentially insulated flat plate with a free-stream Mach number of 3.03 and a Reynolds number of approximately 210,000 based on boundary-layer thickness.

SYMBOLS

a	speed of sound, ft/sec
C_p	pressure coefficient, $\dfrac{p-p_\infty}{q_\infty}$, dimensionless
c_p	specific heat at constant pressure, Btu/lb °F
c_v	specific heat at constant volume, Btu/lb °F
H	boundary-layer-shape parameter, $\dfrac{\delta^*}{\theta}$, dimensionless
I_w	wire current, amp

M Mach number, $\frac{u}{a}$, dimensionless

p static pressure, lb/sq ft

p_t total pressure, lb/sq ft

q dynamic pressure, lb/sq ft

R_e equilibrium resistance of wire with no current flow, ohms

R_w resistance of wire with current flow, ohms

R_δ Reynolds number, $\frac{u_\infty \rho_\infty \delta}{\mu_\infty}$, dimensionless

T static temperature, °R

T_t total temperature, °R

t time, sec

u velocity parallel to plate, ft/sec

x distance along plate from leading edge, ft

y distance normal to plate, ft

γ ratio of specific heats, $\frac{c_p}{c_v}$, dimensionless

δ boundary-layer thickness, ft

δ^* boundary-layer displacement thickness, ft

θ boundary-layer momentum thickness, ft

η_r recovery factor, $\frac{T_w - T_\infty}{T_t - T_\infty}$ dimensionless

μ viscosity, lb-sec/sq ft

ρ mass density, slugs/cu ft

SUBSCRIPTS

∞ free-stream conditions

w conditions on plate surface except for symbols I_w and R_w

SUPERSCRIPT

$'$ conditions downstream of a normal shock

TEST EQUIPMENT

The value of the data obtained in a detailed experimental program depends on how the experiment is conducted and how the results are analyzed. For this reason, relatively detailed accounts of the test equipment, experimental procedure, and data reduction are included in this report to provide the reader with an accurate knowledge of what was done to derive the final results.

8- BY 8-INCH SUPERSONIC NOZZLE

The 8- by 8-inch supersonic nozzle is a nonreturn, continuous-flow type and has rigid nozzle blocks for producing a nominal test-section Mach number of 3. The Reynolds number range obtainable is from 2 million to 14 million per foot.

The nozzle is a standard two-dimensional DeLaval type with the nozzle-block contours symmetrical about the horizontal plane containing the axial center line of the test region. The test region has a constant width of 8 inches and a nominal height of 8 inches. The test-section length is approximately 16 inches. The air flow through the nozzle is sealed from the atmosphere by solid rubber seals compressed between the nozzle blocks and the side walls.

Air is supplied to the nozzle by centrifugal compressors at a maximum pressure of 6 atmospheres absolute. The absolute humidity of the air is maintained at a value below 0.0001 pound of water per pound of air by passing the air

from the compressors first through an aftercooler and then through a silica gel dryer. The total temperature of the supply air is approximately 65° Fahrenheit.

FLAT PLATE AND MOTION MECHANISM

The simplest and most accurate method of obtaining data from the X-ray densitometer was to translate the flat plate relative to a fixed X-ray beam. Therefore, a motion mechanism for the flat plate was constructed and all surveys were made by moving the plate relative to fixed probes. The boundary-layer thickness was on the order of ⅕ inch and no noticeable changes in boundary-layer characteristics occurred while the plate was being translated. A photograph of the flat plate and its motion mechanism is shown in figure 1.

Flat plate.—The solid steel plate was supported in the vertical direction by three Invar struts extending from the motion mechanism. It was restrained in the streamwise and transverse directions at the downstream end by a strut which extended through the tunnel side walls. Figure 2 is a view of the plate in the tunnel, and figure 3 is a sketch showing the principal plate dimensions and thermocouple and pressure orifice locations. The fence on each side of the plate prevented the flow of air from the relatively high-
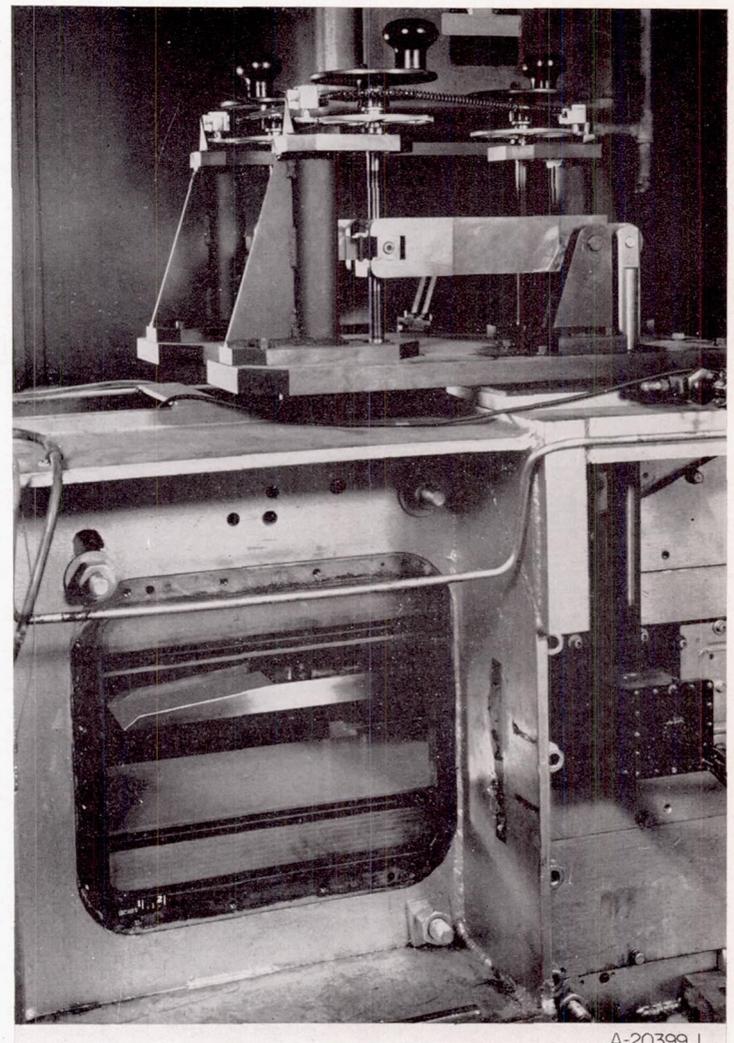

A-20399.1

FIGURE 1.—General arrangement of flat-plate motion mechanism and flat plate in test region of 8- by 8-inch supersonic nozzle.

Figure 2.—Photograph of flat plate in test region with pitot probe installed at survey station.

Figure 3.—Sketch of flat plate.

pressure area on the top to the boundary-layer survey side on the bottom. In order to get as thick a turbulent boundary layer as possible at the survey station (which was 9 inches from the leading edge), a boundary-layer trip was installed 1 inch from the leading edge. The trip consisted of a row of cylindrical rods which protruded perpendicularly to the plate surface.

Motion mechanism.—The motion mechanism consisted of a tripod arrangement in which each leg of the tripod was an Invar strut connected to the flat plate. The other end of each of these legs was then pinned to individual lever arms and lead screws. The lever arm had approximately a 5 to 1 ratio and the lead screw was ⅝ inch in diameter and had 40 threads per inch. Each lead screw was driven by a hand wheel and was also geared to a counter. Each lead screw could be operated independently or all could be operated together by a ladder chain and sprockets. One count on the counter represented 0.0001 inch of plate movement and the maximum amount of backlash ever recorded was 0.0007 inch.

PITOT PROBE

The pitot probe was constructed from 0.028-inch outside diameter hypodermic tubing. The end was machined and flattened to form an opening approximately 0.001 inch high and 0.030 inch wide. The wall thickness at the end was approximately 0.001 inch. This probe according to reference 1 should have negligible interference effects on the boundary layer. The probe was supported by a rigid structure which was in turn bolted to the lower nozzle block.

X-RAY DENSITOMETER

The X-ray instrumentation used in these tests was essentially the same as that described in reference 5 except for the following modifications. A new X-ray tube which produced only one source of X-rays was used. Also, electronic counters were used to count the pulses emitted by the Geiger-Mueller tubes (hereafter referred to as G-M tubes) instead of the ratio meter. The G-M tubes and the X-ray tube again used 0.001-inch-thick cellophane windows as described in reference 5.

The X-rays generated at the tungsten target of the X-ray tube were permitted to travel in two paths—one through the reference chamber to the reference G-M tube and the other through the tunnel (perpendicular to the air flow) to the tunnel G-M tube. The reference X-ray beam passed through a variable-area slit to permit adjustment of the intensity of the reference beam to a value near that of the tunnel X-ray beam. The reference chamber was always pumped to a pressure less than 100 microns so that a negligible absorption of X-rays resulted between the X-ray tube and the reference G-M tube.

The tunnel X-ray beam first passed from the source through a slit whose dimensions were 0.001 inch by 0.100 inch at one tunnel side wall, then through the tunnel and another slit of the same dimensions at the other side wall, and finally to the tunnel G-M tube. Since the X-ray beam was not truly collimated, an experimental check was made to determine whether an appreciable percentage of scattered X-rays was being received by the tunnel G-M tube. Because no appreciable scattering was detected, the effective size of the X-ray beam is believed to have been approximately 0.001 inch high and 0.100 inch wide. The beam was carefully alined with the plate surface so that it was parallel within 0.0006 inch over the 4-inch plate width.

HOT-WIRE PROBE

The hot-wire probe consisted of a 0.0003-inch-diameter tungsten wire spot welded to the tips of two needles spaced about 0.100 inch apart (see fig. 4). The needles were cast in a lucite body which was in turn supported by a rigid strut from the bottom of the wind tunnel in a manner similar to the pitot probe. After the tungsten wire had been welded to the needles, the excess material was removed so that the maximum thickness at the tip was only 0.001 inch. The probe was inclined at an angle of approximately 18° relative to the plate surface in order to get the wire as close to the plate surface as possible and also to reduce the disturbances resulting from the insertion of the needles and wire into the boundary layer. The wire was alined by visual means so that it was parallel to the plate surface within ±0.0005 inch over the length of wire.
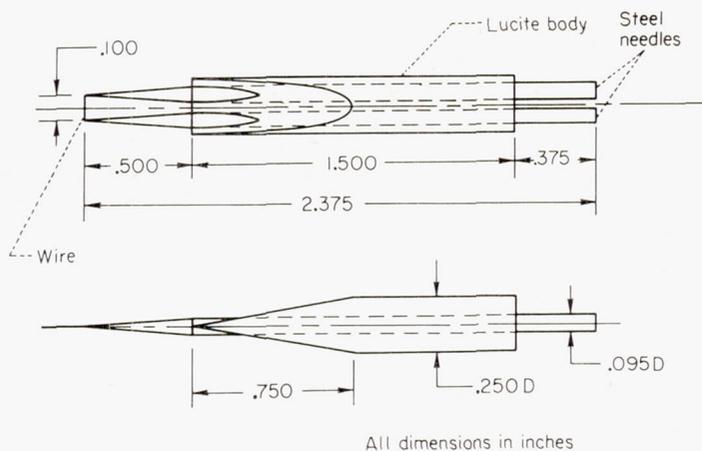
FIGURE 4.—Wire probe.

The wire was heated by passing electrical current through it from a regulated direct current supply. The wire resistance was determined from a standard Wheatstone bridge arrangement in which the tungsten wire was one leg of the bridge. The wire current was determined from the measurement of the voltage across a precision 10-ohm resistor that was connected in series with the wire.

COLD-WIRE PROBE

The cold-wire probe was the same as the hot-wire probe except that no heating current was passed through the wire. The cold-wire resistance (no current flow in wire) was determined by extrapolation of resistances obtained with very low currents through the wire.

EXPERIMENTAL PROCEDURE AND DATA REDUCTION

All the surveys through the turbulent boundary layer were conducted 9 inches downstream of the leading edge of the plate and the plate was moved relative to the fixed probes and X-ray beam. The free-stream Mach number was 3.03 and the free-stream Reynolds number was maintained at 13.6 million per foot. Steady-state conditions of plate pressure and temperature were always established before test data were recorded.

PITOT SURVEY

Pitot pressures were recorded on a standard mercury manometer for various distances of the probe from the plate surface. The measured pitot pressure was assumed to be the true pitot pressure at the center line of the probe opening. The distance between the center line of the probe opening and the plate surface was determined from the recorded counter reading, a calibration of the flat plate motion mechanism as a function of counter reading, and the zero reference distance at which the probe tip contacted the plate surface. This zero reference distance was determined by visual, minimum impact pressure, and electrical-contact methods. The value determined from the minimum impact-pressure method is the initial point at which no further change in pitot pressure occurs when the plate is translated toward the probe. It was found that the visual and minimum impact-pressure methods gave the same zero reference distance within ±0.001 inch. The accuracy of the electrical-contact method was not as good. Hence,

the former two methods were employed throughout the pitot survey tests.

The pitot data were reduced to a ratio of local to free-stream pitot pressures, p_t'/p_{t_∞}'. The boundary-layer thickness was assumed to be the distance at which this ratio was 0.99. This thickness was 0.184 ±0.002 inch. All boundary-layer distributions presented in this report are plotted as a function of the ratio of distance from the plate surface to this boundary-layer thickness, y/δ.

Since the boundary-layer thickness at the survey station was less than 0.20 inch, no attempts were made to measure a static-pressure distribution. However, the static pressure just outside the boundary layer was computed from pitot-pressure and reservoir-pressure measurements and the use of the standard isentropic and normal-shock equations. This computed static pressure agreed with the measured plate surface static pressure within ±0.5 percent which was the amount of experimental scatter. An examination of schlieren photographs indicated total head losses through the bow shock waves of less than 0.5 percent. It was then felt justifiable to assume that the static pressure was constant through the boundary layer.

X-RAY SURVEY

As was pointed out in reference 5, X-rays that have longer wave lengths are more readily absorbed in air than those with shorter wave lengths. Longer wave lengths are produced when lower anode voltages are used on the X-ray tube. However, lowering the anode voltage also reduces the number of quanta produced and, as a result, increases the time required to obtain a time-average value of the intensity of the X-ray beam. Therefore, depending on the particular experimental conditions and the accuracy required for the tests, an anode voltage has to be determined which yields the required accuracy within a reasonable period of time. For these tests concerning the turbulent boundary layer, an anode voltage of 3.20 kilovolts and an emission current of 40 milliamperes (the maximum obtainable with the present equipment) resulted in counting rates on the order of 2000 counts per minute. With these operating conditions, the acceptably short counting interval of 5 minutes was required to obtain a time-average value of intensities which yielded density measurements accurate to approximately ±2 percent. Background count of about 15 counts per minute was considered to be negligible. The G-M tube voltages were maintained between 1100 and 1300 volts, depending on the plateau region for each tube.

The calibration of the X-ray densitometer was conducted with the equipment mounted on the tunnel and after the X-ray beam had been alined with the plate. Hence, no physical movement of the equipment was required between the calibration and the actual density measurements in the boundary layer.

The calibration required recording the ratio of intensities of the tunnel X-ray beam to the reference X-ray beam as a function of the test-section density-path-length [2] with no

---

[2] Density-path-length is defined as the product of average density between two points and the distance between the two points. In this case the distance between the two points is the distance between the cellophane windows on the X-ray tube and G-M tube.

air flow in the tunnel. Since the reference X-ray beam passed through a channel of negligible density, the reference-beam intensity was essentially constant. Only small variations occurred due to changes in quanta production in the X-ray tube. The test-section density was varied by simply changing the test-section pressure. The test-section pressure was changed by the use of vacuum pumps connected to the exhaust piping from the wind tunnel. The air temperature stabilized at room temperature within 1 minute after a pressure change. The calibration of the X-ray densitometer yielded a linear relationship between the logarithm of the intensity ratio and the density-path-length.

At small angles of incidence X-rays may be reflected rather than absorbed in the surface of a steel plate. A reflection check was made by moving the plate toward the X-ray beam while a constant density-path-length was maintained in the test region. When the center line of the beam was approximately 0.005 inch from the surface, the intensity of the beam indicated by the tunnel G-M tube started to increase. The intensity increased as the plate was moved closer to the beam until a maximum value was reached at about 0.001 inch from the plate. The maximum increase in intensity varied between 10 and 15 percent and considerably more scatter in data resulted than when there were no plate reflections. It was felt that no reasonable attempts could be made to correct density measurements when reflected X-rays were involved; hence, no density measurements were made at points less than 0.005 inch from the plate surface.

The X-ray survey was conducted by moving the plate relative to the fixed X-ray beam. The zero reference distance was determined from the point at which the X-ray beam was cut off by the plate. This method proved to be very satisfactory and the distance from the plate surface to the center line of the X-ray beam is accurate within ± 0.001 inch.

Since the free-stream density was known at all times (assuming isentropic flow through the nozzle), the density profile through the boundary layer was determined from the change in density-path-length from the free stream to a point in the boundary layer. This change in density-path-length was, of course, derived directly from the change in X-ray beam intensities and the calibration. A gradual change in the intensity of the X-ray beam in the free stream was noted as the run proceeded. Since no actual change in reservoir conditions was recorded, the change of intensity is believed to have resulted from a slight shifting of the tunnel walls as they cooled. It was necessary to check the intensity of the X-ray beam in the free stream periodically to correct for physical movements of the tunnel.

In order to convert the measured change of density-path-length to the change in density on the center line of the plate, both the path length and average density relative to the density at the center line had to be determined. This was accomplished by making pitot surveys at several spanwise stations. The total temperature and static pressure being assumed constant through the boundary layer, these pitot data were then converted to a ratio of local to free-stream density. A plot of this density ratio as a function of spanwise distance from the center line of the plate permitted the graphical determination of the ratio of center-line density to average density at various distances perpendicular to the plate surface. The path length was the distance between the points on each side of the plate at which the free-stream density was just reached. Except for the regions near the edges of the plate, very little spanwise variation in density occurred. Therefore, the ratio of center-line density to average density over the path length is essentially a tip correction. This tip correction varied from 0.97 near the outer edge of the boundary layer to 0.95 near the surface of the plate.

HOT-WIRE AND COLD-WIRE SURVEYS

The wire surveys were conducted in the same manner as the pitot survey; that is, the plate was moved relative to the fixed probe located at the center line of the plate. Each hot-wire probe was calibrated in the free stream by recording the power dissipated from the wire while varying the free-stream Reynolds number (the Mach number remained essentially constant). The overheat ratio $(R_w - R_e)/R_e$ was maintained at 0.7. Each calibration yielded a linear variation of power dissipation as a function of the square root of of mass flow, $\sqrt{\rho u}$.

The boundary-layer survey consisted of performing the following steps at each point in the boundary layer:
1. Determining the cold resistance, R_e
2. Computing the hot-wire resistance, R_w, for an overheat ratio of 0.7
3. Recording the wire current, I_w, which yielded the computed hot-wire resistance.

These data were then reduced to a ratio of local to free-stream mass flow, $\rho u/\rho_\infty u_\infty$, as a function of y/δ by the use of the calibration curve. The zero reference distance for this survey was again determined by visual means.

In order to reduce the cold-wire-resistance measurements to total temperatures, the recovery factor of the wire was determined from (a) the known resistance and temperature with no air flow, (b) the measured resistance with air flow and known reservoir temperature, and (c) the thermal resistivity of tungsten wire. A ratio of wire temperature to reservoir temperature of 0.970 ± 0.002 resulted at a Mach number of 3.03. This agrees with data from Kovasznay (ref. 6) for 0.003-inch-diameter wires at lower supersonic Mach numbers. Since local Mach numbers in the surveyed portion of the boundary layer were always greater than 1, it was assumed that this temperature ratio was constant.

RESULTS AND DISCUSSION

The flow over the flat plate was first checked by measuring the pressure distribution and recovery-factor distribution along the center line of the plate. The results are shown in figure 5. The adverse pressure gradient at the survey station is approximately a 1-percent increase in static pressure per inch of plate. The recovery factors along the plate at points more than 4 inches from the leading edge compare favorably with data for a fully turbulent boundary layer on an insulated plate from reference 7 at Mach number of 2.4. Spanwise measurements 1.25 inches on each side of the center

(a) Pressure distribution.
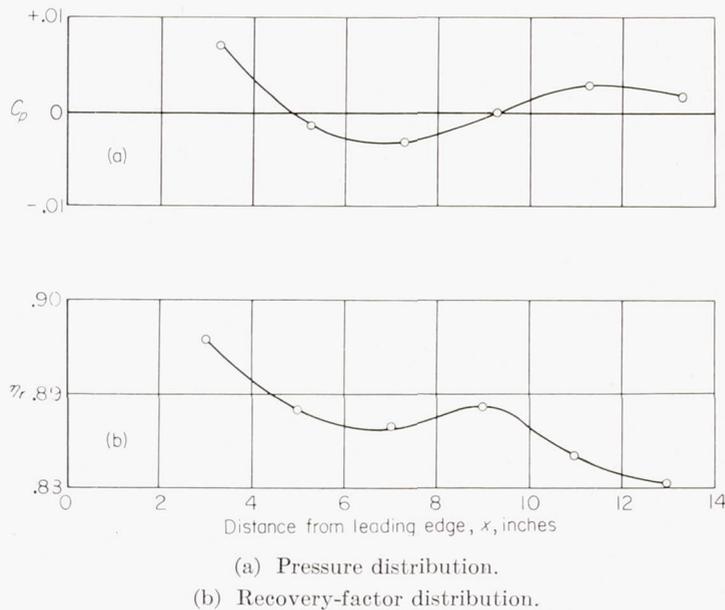
(b) Recovery-factor distribution.

FIGURE 5.—Surface-pressure and recovery-factor distributions along the center line of the flat plate.

line of the plate at a distance of 9 inches from the leading edge yielded a maximum increase in pressure of 2 percent and a maximum increase in recovery factor of 0.1 percent. A schlieren photograph of the boundary layer is presented in figure 6.

The results of the pitot, X-ray, cold-wire, and hot-wire surveys are shown in figures 7 through 10, respectively. These data are from a number of tests and the scatter shown is typical for each surveying instrument. The data points shown at y/δ equal to zero were, of course, obtained from pressure and temperature data on the plate surface. The root mean square of the deviations of data points from the faired curves in figures 7 through 10 are as follows:

Parameter	RMS of deviations
p_t'/p_{t_∞}'	0.012
ρ/ρ_∞	.013
$(T_t - T_{t_\infty})/T_{t_\infty}$	.001
$\rho u/\rho_\infty u_\infty$	.008
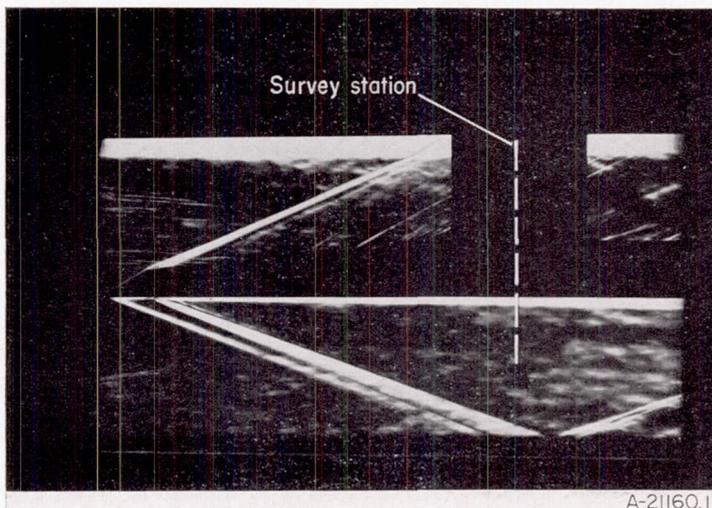
FIGURE 6.—Schlieren photograph of turbulent boundary layer on the flat plate.

It should be noted that the total temperature distribution in figure 9 indicates a relatively large total-temperature gradient near the plate surface. On the other hand, for values of y/δ greater than 0.03, the local total temperature deviates from the free-stream total temperature by less than 3 percent.

Now we wish to check the reliability of the data presented in figures 7 through 10 and hence, in turn, the methods by which they were obtained. This will be done by use of various combinations of the data to obtain the same properties in the boundary layer. Mach number is especially convenient to work with and has been chosen for analysis.
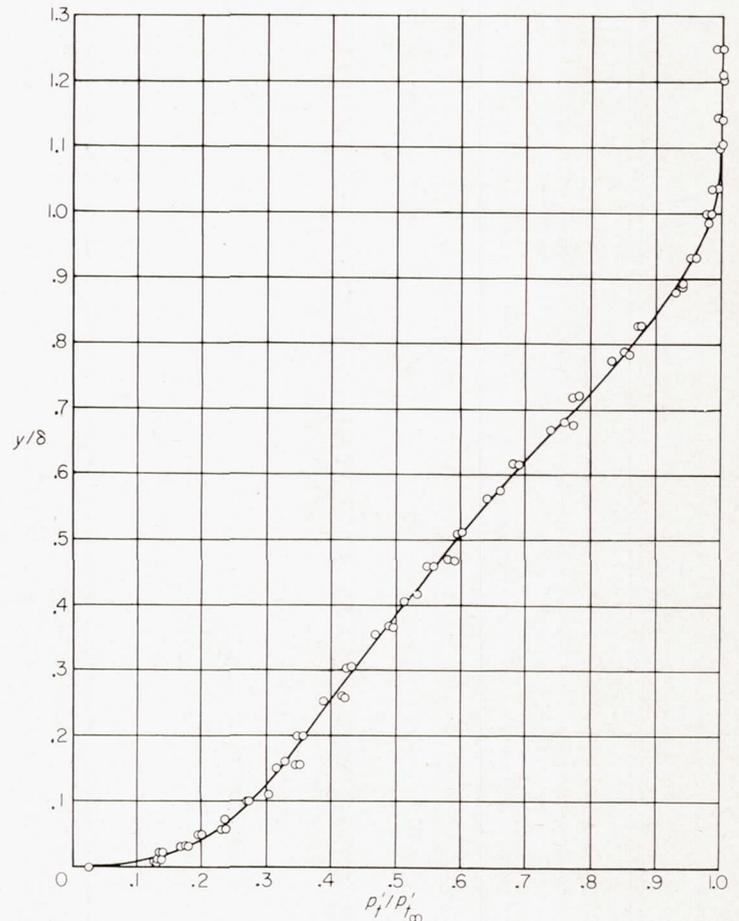
FIGURE 7.—Pitot-pressure distribution through the turbulent boundary layer from pitot-probe measurements.

MACH NUMBER DISTRIBUTIONS

It has been shown earlier in this report that the static pressure through the boundary layer could be considered constant. This fact and the assumption that air behaves as a perfect gas are used in the computation of Mach number by the following four methods.

Method 1.—Mach number was obtained directly from the pitot pressure data (fig. 7) and the Rayleigh pitot formula

$$\frac{p_t'}{p} = \left(\frac{\gamma+1}{2} M^2\right)^{\frac{\gamma}{\gamma-1}} \left[\frac{\gamma+1}{2\gamma M^2 - (\gamma-1)}\right]^{\frac{1}{\gamma-1}} \quad (1)$$

Method 2.—The density and total temperature distributions (figs. 8 and 9) obtained from X-ray and cold-wire sur-
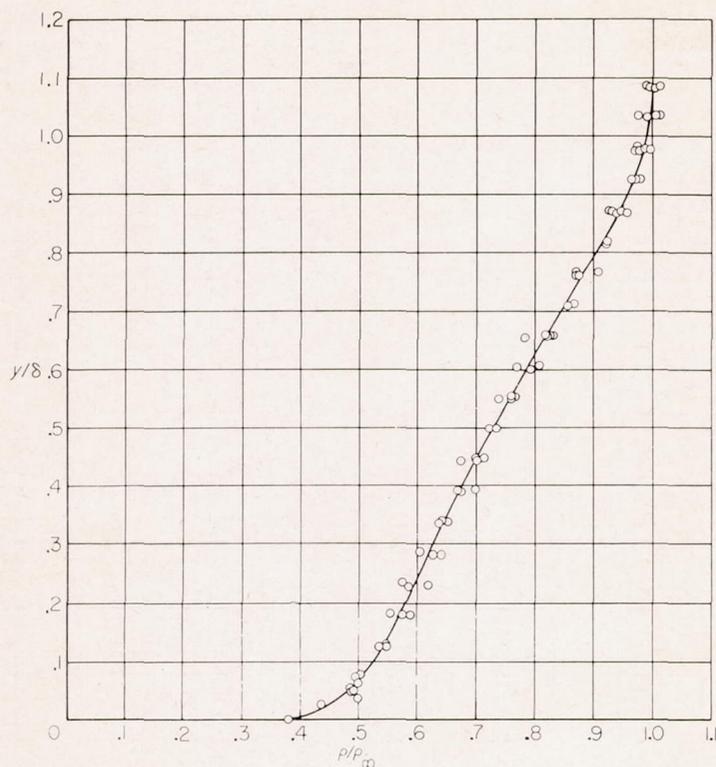
FIGURE 8.—Density distribution through the turbulent boundary layer from X-ray densitometer measurements.

veys were combined to yield a Mach number distribution by using the adiabatic relationship

$$\frac{T}{T_t}=\left(1+\frac{\gamma-1}{2}M^2\right)^{-1}$$

to obtain the equation

$$1+\frac{\gamma-1}{2}M^2=\left(1+\frac{\gamma-1}{2}M_\infty^2\right)\left(\frac{T_t}{T_{t_\infty}}\right)\left(\frac{\rho}{\rho_\infty}\right) \qquad (2)$$

Method 3.—It can be shown that total temperature, mass flow, and Mach number are related by the fourth-degree equation

$$M^2\left(\frac{\gamma-1}{2}M^2+1\right)=M_\infty^2\left(1+\frac{\gamma-1}{2}M_\infty^2\right)\left(\frac{T_t}{T_{t_\infty}}\right)\left(\frac{\rho u}{\rho_\infty u_\infty}\right)^2 \qquad (3)$$

Therefore, cold-wire and hot-wire data (figs. 9 and 10) were combined to yield Mach number.

Method 4.—Data from the X-ray and hot wire (figs. 8 and 10) were combined directly. Mach number was then obtained from the equation

$$M=M_\infty\left(\frac{\rho u}{\rho_\infty u_\infty}\right)\left(\frac{\rho}{\rho_\infty}\right)^{-\frac{1}{2}} \qquad (4)$$

The Mach number distributions resulting from each of the four methods are presented in figure 11. Note that the distributions using the pitot data and the combined X-ray and cold-wire data are very nearly the same; whereas the other two distributions which used hot-wire data indicate appreciably higher Mach numbers over a large portion of the boundary layer.
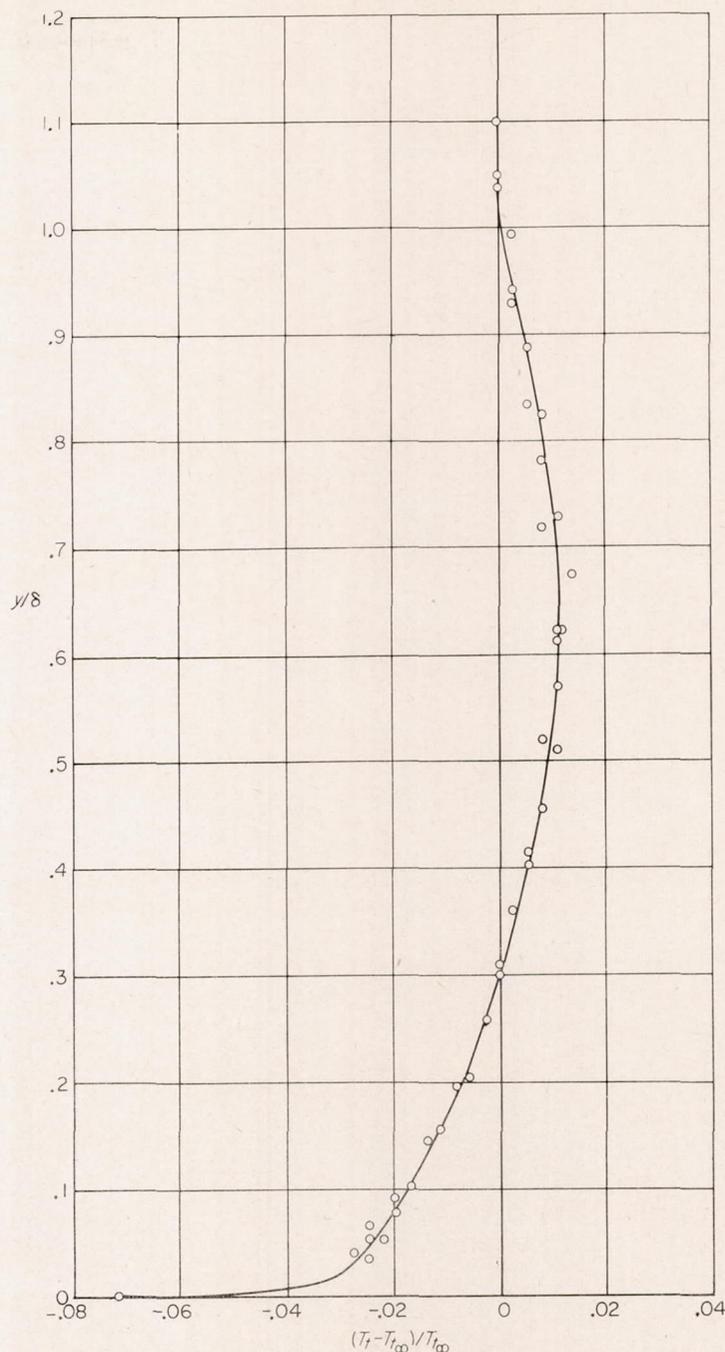
FIGURE 9.—Total-temperature distribution through the turbulent boundary layer from cold-wire-resistance measurements.

Supporting evidence of this discrepancy was recorded in an independent test performed by Mr. Howard Stine and Mr. Warren Winovich in the Ames 1- by 3-foot supersonic wind tunnel. Their pitot, hot-wire, and cold-wire measurements were made in the tunnel side-wall boundary layer which was approximately 2.84 inches thick and the free-stream Mach number was 1.95. The Mach number distributions are shown in figure 12. Although these data were incidental to another test and, therefore, only a few data points were obtained, there is little doubt that the trend is the same as that shown in figure 11.

It is not now obvious which of the Mach number distributions in figure 11 may be considered to be the more reliable. Therefore, it was decided that another property should be
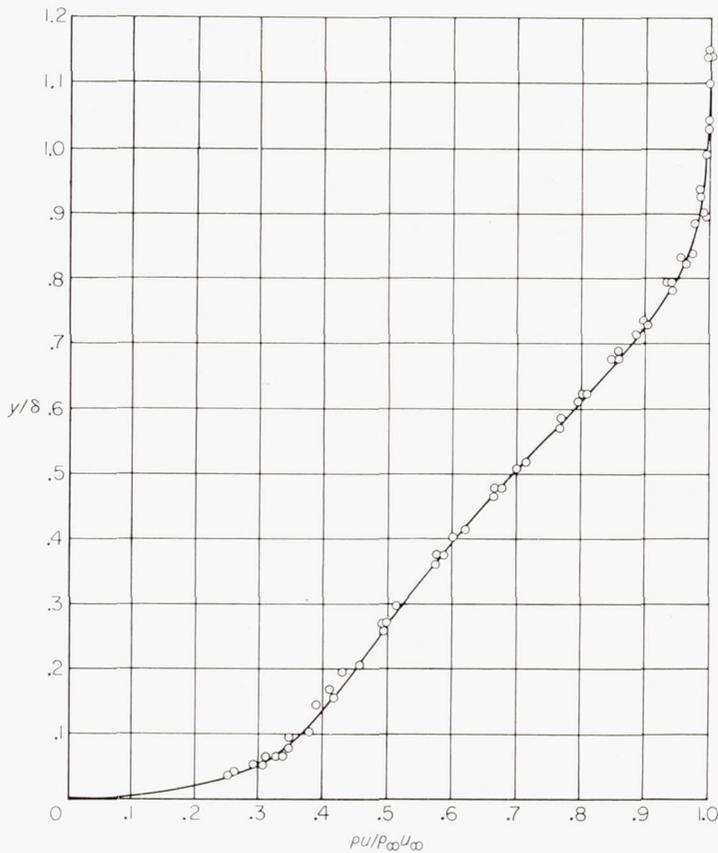
FIGURE 10.—Mass-flow distribution through the turbulent boundary layer from hot-wire measurements.
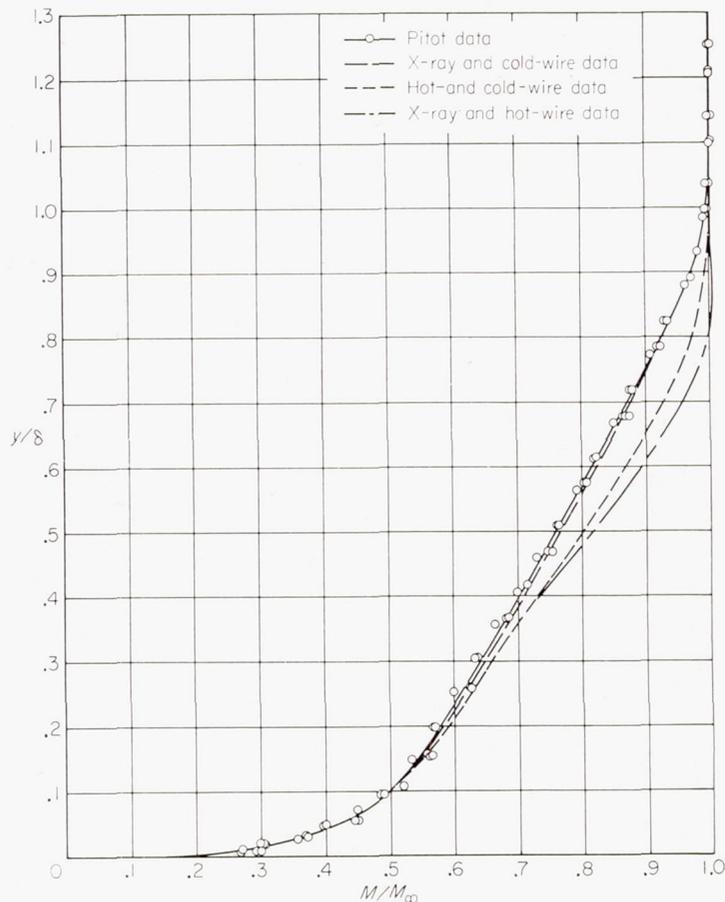

FIGURE 11.—Mach number distributions through the turbulent boundary layer from pitot, X-ray, cold-wire, and hot-wire data.
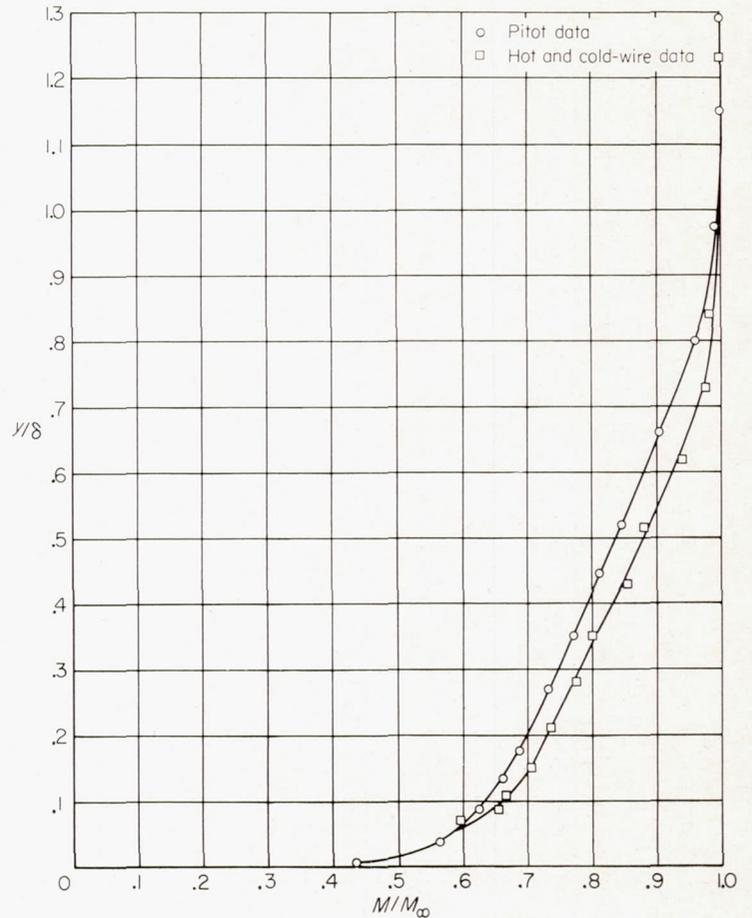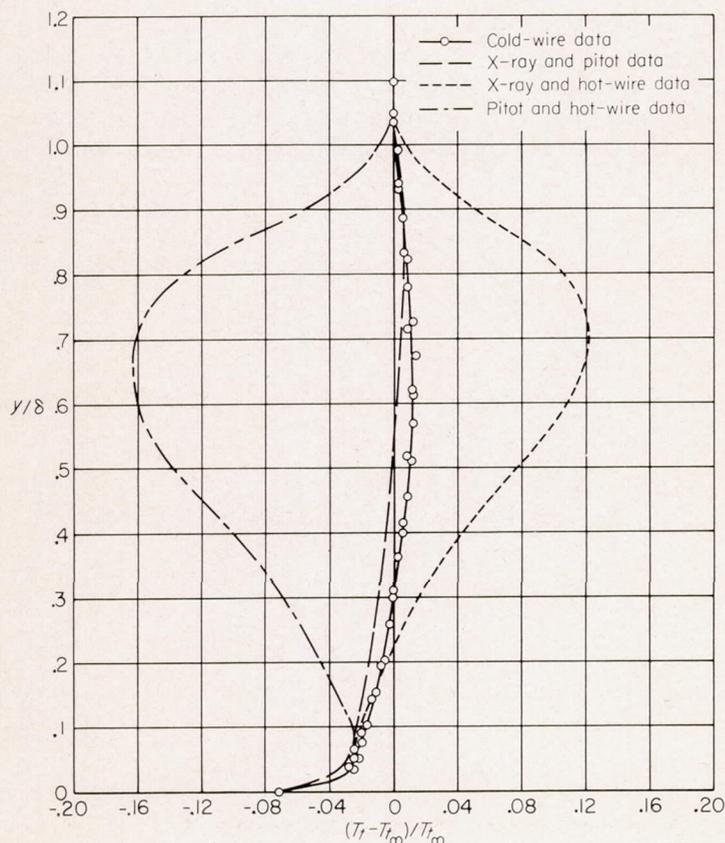

FIGURE 12.—Mach number distributions through the turbulent boundary layer on the side wall of the Ames 1- by 3-foot supersonic wind tunnel from pitot, cold-wire, and hot-wire data; $M_\infty = 1.95$, $\delta = 2.84$ inches.

computed which would permit further evaluation of the basic data.   Total temperature was chosen.

TOTAL TEMPERATURE DISTRIBUTIONS

The assumptions of constant static pressure and the perfect gas law were also used to obtain total temperature.

Method 1.—Total temperature resulted directly from the cold-wire-resistance measurements as described in the section "Experimental Procedure and Data Reduction."

Method 2.—Total temperature was obtained from the combined pitot and X-ray data (figs. 7 and 8) and equation (2) revised to read

$$\frac{T_t - T_{t_\infty}}{T_{t_\infty}} = \frac{1 + \frac{\gamma - 1}{2} M^2}{1 + \frac{\gamma - 1}{2} M_\infty^2} \frac{1}{\rho / \rho_\infty} - 1 \tag{5}$$

Local Mach number was in this case obtained from the pitot data and equation (1).

Method 3.—Total temperature was obtained from the combined X-ray and hot-wire data (figs. 8 and 10) and the energy equation for the adiabatic flow of a perfect gas.

$$c_p T + \frac{u^2}{2} = c_p T_t \tag{6}$$

This equation can be rewritten as

$$\frac{T_t - T_{t_\infty}}{T_{t_\infty}} = \frac{T}{T_{t_\infty}} + \frac{u_\infty^2}{2c_p T_{t_\infty}} \left(\frac{u}{u_\infty}\right)^2 - 1 \tag{7}$$

The temperature ratio, T/T_{t_∞}, is obtained from the X-ray data and the known free-stream Mach number by the equation

$$\frac{T}{T_{t_\infty}} = \left[\left(1 + \frac{\gamma-1}{2}M_\infty^2\right)\left(\frac{\rho}{\rho_\infty}\right)\right]^{-1} \tag{8}$$

and u/u_∞ is obtained from

$$\frac{u}{u_\infty} = \frac{\rho u/\rho_\infty u_\infty}{\rho/\rho_\infty} \tag{9}$$

Method 4.—Total temperature was obtained from the combined pitot and hot-wire data (figs. 7 and 10) and equation (7) where

$$\frac{T}{T_{t_\infty}} = \left(\frac{\rho u/\rho_\infty u_\infty}{M/M_\infty}\right)^2 \left(1 + \frac{\gamma-1}{2}M_\infty^2\right)^{-1} \tag{10}$$

and

$$\frac{u}{u_\infty} = \frac{(M/M_\infty)^2}{\rho u/\rho_\infty u_\infty} \tag{11}$$

The total-temperature distributions which resulted from each of the four methods are presented in figure 13. It can clearly be seen that the combined X-ray and pitot data yield a total temperature distribution very near that from

FIGURE 13.—Total-temperature distributions through the turbulent boundary layer from pitot, X-ray, cold-wire, and hot-wire data.
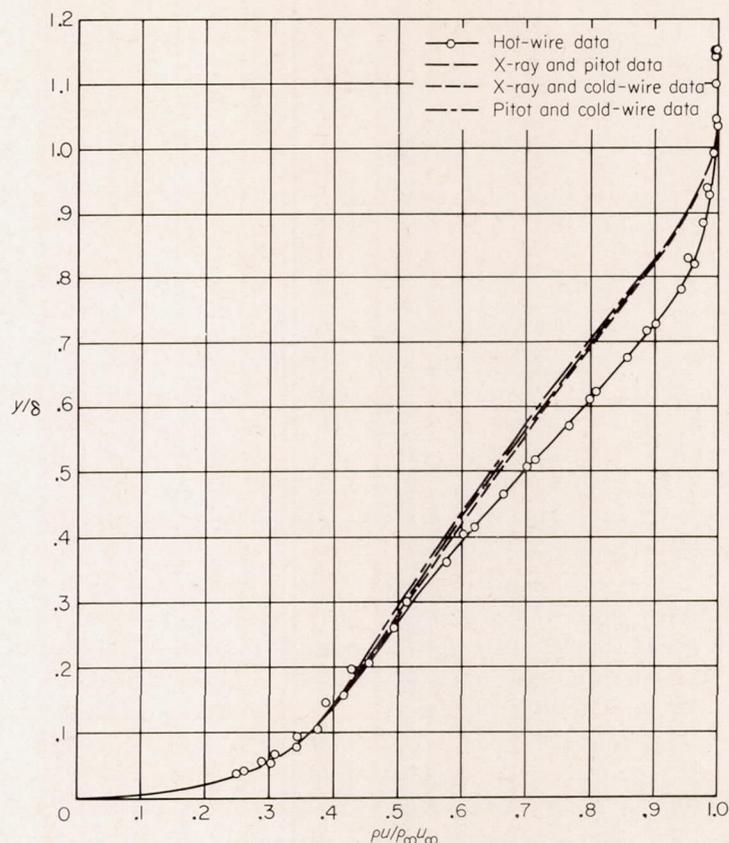
FIGURE 14.—Mass-flow distributions through the turbulent boundary layer from pitot, X-ray, cold-wire, and hot-wire data.

the cold wire. The other two combinations which use hot-wire data yield distributions which deviate considerably from the distribution obtained from the cold wire.

From the foregoing comparisons of Mach number distributions and total-temperature distributions it is clear that the mean-mass-flow data from the hot-wire probe are not consistent with the data from the pitot, X-ray, and cold-wire surveys. The data presented in figure 14 show that the mean mass flow from the hot-wire probe is higher than those from the combined pitot, X-ray, and cold-wire data over a large portion of the boundary layer. Similar tests in the subsonic turbulent boundary layer have, however, yielded relatively good agreement between pitot and hot-wire data (see ref. 8). Therefore, the following study was made to determine a possible explanation for the difference between results obtained in the subsonic boundary layer of reference 8 and the present supersonic turbulent boundary layer.

MASS-FLOW DISCREPANCY

Assume at any time, t, that the instantaneous values of density and velocity, ρ^* and u^*, are defined as

$$\rho^* = \rho + \Delta\rho$$

and

$$u^* = u + \Delta u$$

where ρ and u are independent of time and

$$\frac{1}{t}\int_0^t \Delta\rho\, dt = \frac{1}{t}\int_0^t \Delta u\, dt = 0$$

The mass flow at any instant is then

$$\rho^*u^* = (\rho + \Delta\rho)(u + \Delta u) = \rho u + u\Delta\rho + \rho\Delta u + \Delta\rho\Delta u$$

The mean mass flow is then

$$\frac{1}{t}\int_0^t \rho^*u^*dt = \frac{1}{t}\int_0^t \rho u\,dt + \frac{1}{t}\int_0^t u\Delta\rho\,dt + \frac{1}{t}\int_0^t \rho\Delta u\,dt + \frac{1}{t}\int_0^t \Delta\rho\Delta u\,dt$$

$$= \rho u + 0 + 0 + \frac{1}{t}\int_0^t \Delta\rho\Delta u\,dt \qquad (12)$$

For the case of the subsonic boundary layer where $\Delta\rho$ is negligible, the last term of equation (12) must also be negligible. However, for the supersonic boundary layer, the last term of equation (12) need not necessarily be negligible. This is especially true in the outer portion of the boundary layer where the flow at a given position is characterized by intermittency (see ref. 9).

Heretofore, the analysis of the pitot, X-ray, and cold-wire data has employed the implicit assumption that the last term of equation (12) was zero and that the mean mass flows obtained from the hot-wire data are numerically equal to those derived from the pitot, X-ray, and cold-wire data. It now appears possible that the differences shown in figures 11, 13, and 14 have resulted from the ability of the hot wire to indicate the component of mass flow represented by the last term of equation (12). The ability of a hot wire to follow velocity and density fluctuations depends on the heat lag characteristics of the wire. Therefore, one might expect that different mean mass flows could be obtained in the same stream by using various sizes of wires, and corrections to the hot-wire data would be required to obtain true mean mass flows in supersonic turbulent boundary layers.

The pitot probe, X-ray densitometer, and cold-wire probe yielded mean values of pitot pressure, density, and total temperature which produced consistent distributions of Mach number, total temperature, and mass flow throughout the boundary layer. However, mean mass flows computed from the pitot, X-ray, and cold wire data, do not include the increment of mean mass flow represented by the last term of equation (12). Hence, these mass flows can be in error for a supersonic turbulent boundary layer.

EFFECTS OF ASSUMING THE TOTAL TEMPERATURE CONSTANT

The pitot tube has been perhaps the most commonly employed boundary-layer survey instrument. It would be desirable, therefore, to check the accuracy of the assumption of constant total temperature which is often used to reduce pitot data to various other boundary-layer parameters. Mass-flow defect, momentum loss, and velocity distributions are perhaps the most common parameters and they have, therefore, been chosen for analysis. Let us examine mass-flow defect first.

The mass-flow defect was computed using (a) the X-ray and pitot surveys (effects of total-temperature variation are included) and (b) the pitot data and the total temperature assumed constant. These distributions are presented in figure 15. Note that there is almost a negligible difference in the distributions. Also, of course, there is a negligible difference in the displacement thickness obtained by inte-
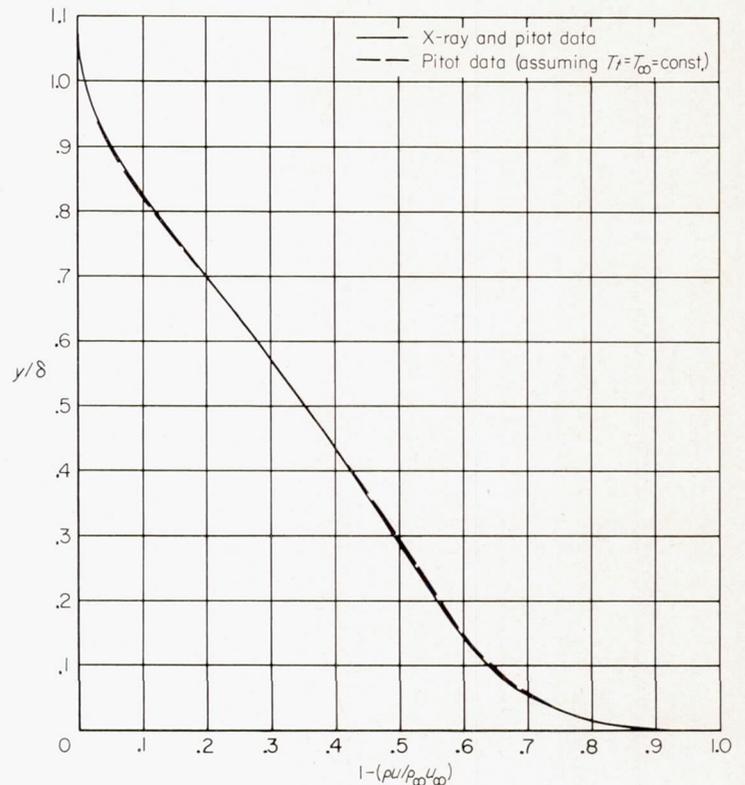

FIGURE 15.—Mass-flow-defect distributions through the turbulent boundary layer.

gration of these distributions. A value of $\delta^*/\delta = 0.350 \pm 0.002$ was obtained from figure 15.

A similar analysis was made for the momentum-loss distributions shown in figure 16. Here the distributions are noticeably different. However, integration of these distributions yielded a momentum thickness according to the combined pitot and X-ray data only about 1-percent greater than that according to the pitot data and assumed constant
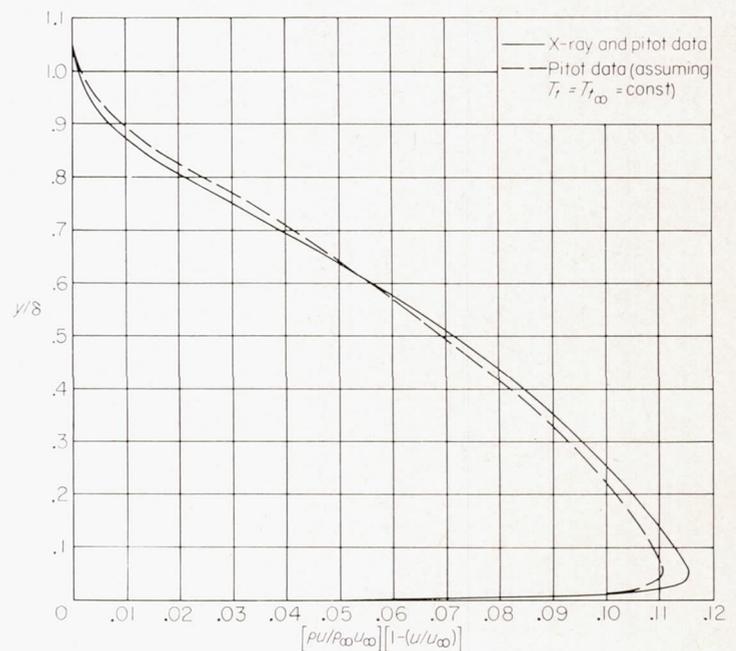

FIGURE 16.—Momentum-loss distributions through the turbulent boundary layer.
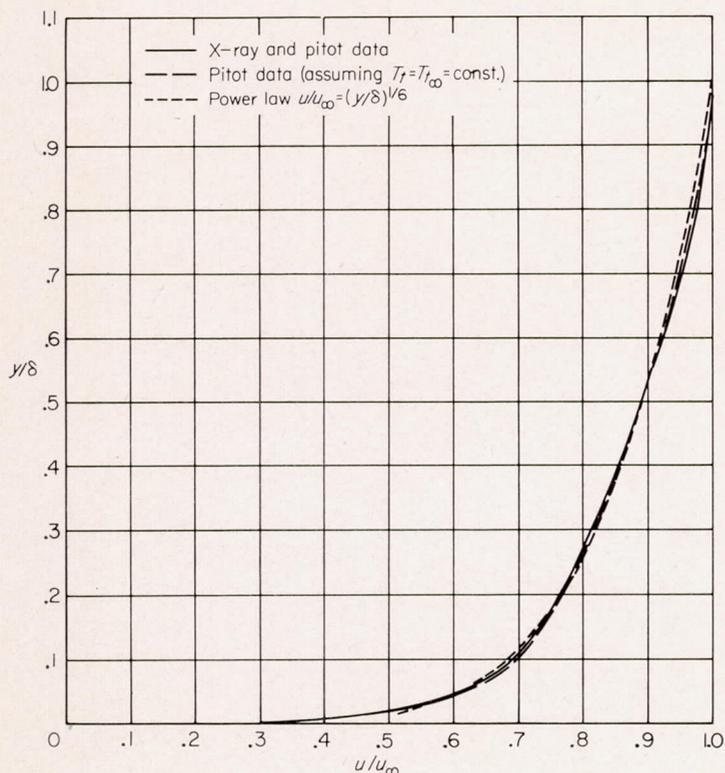
FIGURE 17.—Velocity distributions through the turbulent boundary layer.

total temperature. The value for the former case was $\theta/\delta = 0.0642 \pm 0.0002$. The shape parameter for these tests was then $H = \delta^*/\theta = 5.45$.

The velocity distributions were computed for the two cases and are shown in figure 17. It can be seen that the assumption of constant total temperature yields an almost negligible change in the velocity profile.

Theoretical analysis of turbulent boundary layers often assumes a power law distribution of velocity. The one-sixth power law was computed and is also shown in figure 17. For the region $0.03 < y/\delta < 1.0$ the one-sixth power law deviates from the experimental velocity distribution by not more than ± 2 percent of the free-stream velocity.

CONCLUSIONS

The following conclusions were drawn from this experimental investigation of a turbulent boundary layer on a flat plate at a free-stream Mach number of 3.03.

1. The values of mean pitot pressure, mean density, and mean total temperature obtained from the pitot probe, X-ray densitometer, and cold-wire probe combined to pro-duce consistent distributions of mean Mach number, mean total temperature, and mean mass flow throughout the boundary layer. However, mean mass flows computed from these data do not include the effects of combined density and velocity fluctuations and, hence, they can be in error for the supersonic turbulent boundary layer.

2. The hot-wire probe indicated values of mean mass flow over the outer portion of the boundary layer that were higher than the values obtained from the pitot, X-ray, and cold-wire surveys. This result was confirmed in an independent test performed at a Mach number of 1.95 in the Ames 1- by 3-foot supersonic wind tunnel. It is suggested that corrections to hot-wire data may be required to obtain true mean mass flows in turbulent supersonic boundary layers.

3. The assumption of constant total temperature through the boundary layer yields negligible errors in displacement and momentum thicknesses. The error in velocity distribution computed from pitot data and assumed constant total temperature is also negligible. The one-sixth power law was found to agree with the experimental velocity distribution within ± 2 percent.

AMES AERONAUTICAL LABORATORY
NATIONAL ADVISORY COMMITTEE FOR AERONAUTICS
MOFFETT FIELD, CALIF., *Apr. 19, 1956*

REFERENCES

1. Davies, F. V.: Some Effects of Pitot Size on the Measurement of Boundary Layers in Supersonic Flow. R. A. E. TN No. Aero. 2179, Aug. 1952.
2. Goldstein, S., ed.: Modern Developments in Fluid Dynamics. Oxford Univ. Press, vol. I, ch. VI, Section II, III, 1938, pp. 248–254.
3. Weltmann, Ruth N., and Kuhns, Perry W.: Density Profiles of Subsonic Boundary Layers on a Flat Plate Determined by X-Ray and Pressure Measurements. NACA TN 3098, 1954.
4. Kovásznay, Leslie S. G.: Turbulence in Supersonic Flow. Jour. Aero. Sci., vol. 20, No. 10, Oct. 1953, pp. 657–674, 682.
5. Dimeff, John, Hallett, Ralph K., Jr., and Hansen, C. Frederick: X-Ray Instrumentation for Density Measurements in a Supersonic Flow Field. NACA TN 2845, 1952.
6. Kovásznay, Leslie S. G.: The Hot-Wire Anemometer in Supersonic Flow. Jour. Aero. Sci., vol. 17, No. 9, Sept. 1950, pp. 565–572, 584.
7. Stalder, Jackson R., Rubesin, Morris W., and Tendeland, Thorval: A Determination of the Laminar-, Transitional-, and Turbulent-Boundary-Layer Temperature-Recovery Factors on a Flat Plate in Supersonic Flow. NACA TN 2077, 1950.
8. Laufer, John: Investigation of Turbulent Flow in a Two-Dimensional Channel. NACA Rep. 1053, 1951. (Supersedes NACA TN 2123.)
9. Klebanoff, P. S.: Characteristics of Turbulence in a Boundary Layer With Zero Pressure Gradient. NACA TN 3178, 1954.